HHS Public Access

Author manuscript

Sci Transl Med. Author manuscript; available in PMC 2016 February 18.

Published in final edited form as:

Sci Transl Med. 2015 October 28; 7(311): 311ra171. doi:10.1126/scitranslmed.aac7793.

Mortality factor 4 like 1 protein mediates epithelial cell death in a mouse model of pneumonia

Chunbin Zou[1,*], **Jin Li**[1], **Sheng Xiong**[1], **Yan Chen**[1], **Qin Wu**[1], **Xiuying Li**[1], **Nathaniel M. Weathington**[1,2], **Seung Hye Han**[1], **Courtney Snavely**[1], **Bill B. Chen**[1], and **Rama K. Mallampalli**[1,2,3,*]

[1]Department of Medicine, Acute Lung Injury Center of Excellence, University of Pittsburgh, Pittsburgh, PA 15213, USA

[2]Medical Specialty Service Line, Veterans Affairs Pittsburgh Healthcare System, Pittsburgh, PA 15240, USA

[3]Department of Cell Biology and Physiology, University of Pittsburgh, Pittsburgh, PA 15213, USA

Abstract

Unchecked epithelial cell death is fundamental to the pathogenesis of pneumonia. The recognition of unique signaling pathways that preserve epithelial cell viability may present new opportunities for interventional strategies. We describe that mortality factor 4 like 1 (Morf4l1), a protein involved in chromatin remodeling, is constitutively expressed at low levels in the lung because of its continuous degradation mediated by an orphan ubiquitin E3 ligase subunit, Fbxl18. Expression of Morf4l1 increases in humans with pneumonia and is up-regulated in lung epithelia after exposure to *Pseudomonas aeruginosa* or lipopolysaccharide. In a mouse model of pneumonia induced by *P. aeruginosa*, Morf4l1 is stabilized by acetylation that protects it from Fbxl18-mediated degradation. After *P. aeruginosa* infection of mice, overexpression of *Morf4l1* resulted in lung epithelial cell death, whereas its depletion restored cell viability. Using in silico modeling and drug-target interaction studies, we identified that the U.S. Food and Drug Administration–approved thrombin inhibitor argatroban is a Morf4l1 antagonist. Argatroban inhibited Morf4l1-dependent histone acetylation, reduced its cytotoxicity, and improved survival of mice with experimental lung injury at doses that had no anticoagulant activity. These studies uncover a previously unrecognized biological mechanism whereby pathogens subvert cell viability by

[*]Corresponding author. mallampallirk@upmc.edu (R.K.M.); zouc@upmc.edu (C.Z.).

SUPPLEMENTARY MATERIALS

www.sciencetranslationalmedicine.org/cgi/content/full/7/311/311ra171/DC1

Materials and Methods

Fig. S1. Endotoxin and *P. aeruginosa* increase Morf4l1 protein levels posttranslationally in lung cells.

Fig. S2. Bacterial pathogens trigger Morf4l1 acetylation.

Fig. S3. Effect of Morf4l1 depletion or antagonism on bacterial loads.

Fig. S4. Effect of Morf4l1 depletion or antagonism on the Fas cell death pathway.

Fig. S5. Morf4l1 mediates cell death in pneumonia.

Author contributions: C.Z. conceived the science, oversaw and designed the studies, performed experiments, analyzed the data, and wrote the manuscript; J.L., S.X., Y.C., Q.W., X.L., and C.S. performed experiments and assisted with animal experiments; B.B.C. assisted with the in silico argatroban studies; S.H. assisted with statistical analysis; N.M.W. assisted with writing and editorial revisions; R.K.M. revised the manuscript and assisted C.Z. in the direction of the study.

Competing interests: The authors declare that they have no competing interests.

extending the life span of a cytotoxic host protein. Morf4l1 may be a potential molecular target for non-antibiotic pharmacotherapy during severe pulmonary infection.

INTRODUCTION

Bacterial pneumonia remains a predominant cause of infectious deaths in the United States, and the challenge to effectively treat this illness is compounded by the emergence of multidrug resistant bacterial strains (1). Thus, the identification of new molecular pathways that partake in the pathobiology of severe bacterial infections remains an unmet need. *Pseudomonas aeruginosa* is a well-known nosocomial and opportunistic Gram-negative bacterium causing pneumonia that is associated with high morbidity and mortality. This pathogen very commonly develops multidrug antibiotic resistance and is among the predominant isolates in acute lung injury (ALI), a condition that can occur in people with severe pneumonia (2). The pathogenesis of ALI or its more severe form, acute respiratory distress syndrome (ARDS), is classified into three major phases: inflammation, proliferation, and fibrosis. Cell death is a prominent pathological hallmark observed in the early stages of inflammation associated with both pneumonia and ARDS (3). The mechanisms of cell death during virulent bacterial infections are still not well understood and may be important in devising non–antibiotic-based therapeutic strategies.

Epigenetics is a rapidly evolving field that affects cellular life span involving processes where gene activity is changed without alterations in the DNA sequence. Histone modifications (methylation, acetylation, phosphorylation, etc.) are well-established events that epigenetically regulate gene expression, and recent studies indicate that histone posttranslational modification is modulated by bacterial infection (4). Histone acetyltransferases are a group of well-conserved enzymes in living organisms that catalyze the covalent addition of an acetyl group to lysine residues in histones. More than 90% of chromatin-associated proteins are acetylated, causing changes in chromosomal accessibility, gene expression, and cellular function (5). Some acetyltransferases, such as p300/cyclic adenosine 5′-monophosphate–responsive element–binding protein (CBP) and general control nonderepressible 5 (GCN5), acetylate histones and other proteins to loosen chromatin structure thereby activating gene transcription (6). One protein subunit that associates with acetyltransferases and various transcriptional complexes, called mortality factor on chromosome 4 like protein 1 (Morf4l1) or *Morf*-related genes (*Mrg*) on chromosome 15 (Mrg15), was first cloned as a paralog of the senescence gene product mortality factor on chromosome 4 (Morf4) (7–12). Morf4l1 is a multifunctional protein that modulates cell viability, development, and DNA repair (7–12). However, there appears to be some ambiguity in the biological roles of Morf4l1 regarding cell viability between systems. Targeted disruption of the *Morf4l1* gene leads to growth defects and is lethal in both mice and the nematode *Caenorhabditis elegans* (12–15). Morf4l1-deficient neuronal cells also exhibit defects in proliferation (16, 17). However, overexpression of MRG-1, a *C. elegans* ortholog of Morf4l1, triggers cell death, and *Morf4l1* silencing reduces the ability of the fungal product galectin to mediate apoptosis (12, 18). Thus, the biological role of Morf4l1 requires further study, and factors that control its abundance in cells remain largely unknown.

The cellular ubiquitin proteasomal degradation system regulates the concentration of most cellular proteins including histone modification enzymes; further, acetylation of substrates can compete with ubiquitination to regulate protein abundance and cell function (19). Protein ubiquitination is carefully orchestrated through actions of a series of key enzymes (E1 activating enzyme, E2 conjugating enzyme, and E3 ligase). The last step involving ligation of ubiquitin to its substrate by a ubiquitin E3 ligase is critical because it provides selectivity between an enzyme and substrate in the protein degradation pathway. Thus, E3 ligases may be an opportunity for therapeutic targeting (20). Of the hundreds of E3 ubiquitin ligases, the Skp–Cullin–F-box (SCF) family represents an emerging class of proteins that modulates diverse processes including cellular life span (21). Small molecule antagonists have been developed against the SCF receptor component, the F-box, for preclinical use (20, 22). Indeed, SCF components target some acetyltransferases for their disposal to alter cellular proliferation (23). Although ~70 F-box proteins have been identified in the human genome, the targets for only a few have been well described.

Here, we discovered that in the native state, lung epithelial cell viability is preserved partly because a previously uncharacterized F-box protein, Fbxl18, mediates the disposal of Morf4l1. Disposal of Morf4l1 is both sufficient and required to reduce cell death. *P. aeruginosa* induces the acetylation of Morf4l1 thereby protecting the protein from the destabilizing actions of Fbxl18, leading to the accumulation of Morf4l1, which becomes cytotoxic. Using molecular docking simulation modeling, we identified a small molecule (argatroban) approved by the U.S. Food and Drug Administration (FDA) that tightly binds to Morf4l1 and selectively antagonizes Morf4l1-associated histone acetylation, thus abrogating cytotoxic activity. When administered to an experimental mouse model of ALI, this agent lessened the severity of pulmonary injury and increased mouse survival. These results provide a distinct molecular model for bacterial pneumonia–associated ALI whereby a pathogen, through its stabilizing actions on a cell death effector protein, triggers necrosis of the infected organ. These results also suggest that repurposing of the FDA-approved agent argatroban, which targets Morf4l1, might serve to preserve epithelial cell viability during pulmonary inflammation induced by infection.

RESULTS

Morf4l1 protein expression is elevated in pneumonia

We analyzed lung tissues from patients with pneumonia by immunoblotting for transcriptional regulators (Fig. 1, A and B). Morf4l1 protein was markedly elevated in human pneumonia lung small airway tissues ($n = 8$) compared with lung tissues from uninfected subjects ($n = 5$) ($P = 0.029$). As a control, expression of the transcriptional coactivator CBP was evaluated and was not markedly altered. To confirm this observation, we treated murine lung epithelial cells with lipopolysaccharide (LPS) and observed that Morf4l1 protein expression increased in a dose-dependent manner (Fig. 1C). LPS did not significantly affect total cellular steady-state Morf4l1 mRNA expression (Fig. 1D). Given that the bacterium *P. aeruginosa* is one predominant cause of pneumonia, we co-incubated lung epithelial cells with this pathogen and observed increased Morf4l1 protein levels without alterations in mRNA expression at the multiplicity of infection (MOI) tested (Fig. 1,

E and F). Notably, *P. aeruginosa* infection increased the abundance of histone acetyltransferases including general control nonderepressible 5 (GCN5); however, the pathogen did not increase GCN5 mRNA (fig. S1A). *P. aeruginosa* infection–induced increases in Morf4l1 protein were also observed in human neutrophils and in human endothelial cells, in addition to lung epithelia, but were not observed in human primary macrophages (fig. S1, B and C). Finally, the effects of LPS and *P. aeruginosa* infection on induction of Morf4l1 protein in cells were blocked with LPS from the bacterium *Rhodobacter sphaeroides*, a potent competitive inhibitor of the LPS–Toll-like receptor 4 axis (fig. S1D). Thus, Morf4l1 abundance was increased in both human lungs and lung epithelial cells after bacterial infection with *P. aeruginosa*.

Morf4l1 is a short-lived protein degraded through the ubiquitin proteasome

The protein abundance of transcriptional and chromatin remodeling subunits in cells may be due to altered protein turnover. Morf4l1 is a labile protein in cells with a half-life of about 30 min (Fig. 2, A and B). Morf4l1 degradation is proteasome-dependent because the addition of the proteasome inhibitor MG132 (*N*-carbobenzyloxy-L-leucyl-L-leucyl-L-leucinal) caused accumulation of this cellular protein (Fig. 2A, middle panels), whereas the lysosome inhibitor leupeptin did not affect Morf4l1 protein expression (Fig. 2A, bottom panels). Because proteins selectively degraded through the proteasome are modified by ubiquitination, we mapped putative ubiquitination sites in Morf4l1 and found that K^{143} is the major ubiquitin acceptor site. Mutation of this lysine residue protects Morf4l1 from degradation (Fig. 2C, bottom panels), whereas mutation of the adjacent K^{136} did not affect Morf4l1 degradation (Fig. 2C, middle panels). Morf4l1 polyubiquitination was markedly reduced when we expressed a *Morf4l1* V5-K143R mutant plasmid versus a wild-type *Morf4l1* plasmid in cells (Fig. 2D). In these studies, we coimmunoprecipitated the ectopically expressed Morf4l1 proteins from cell lysates and probed the immunoprecipitates using ubiquitin antibody in immunoblotting studies. These data indicate that Morf4l1 is a labile protein that is degraded through the ubiquitin proteasome pathway after its site-specific polyubiquitination.

SCF^{Fbxl18} degrades Morf4l1

To identify the E3 ubiquitin ligase that mediates Morf4l1 degradation, we screened a library of SCF E3 ligase components and identified that an orphan F-box protein, termed Fbxl18 (SCF^{Fbxl18}), profoundly destabilizes Morf4l1 (Fig. 3A). Cellular expression of *Fbxl18* plasmid was sufficient to mediate Morf4l1 degradation in lung epithelia (Fig. 3B). As a control, the unrelated F-box protein Fbxw18 does not change Morf4l1 protein degradation kinetics. F-box proteins form a complex with Skp1 and Cullin1 to form the SCF E3 ubiquitin ligase complex that binds and ubiquitinates target proteins. In coimmunoprecipitation studies, Fbxl18 specifically interacts with Morf4l1, Skp1, and Cullin1, indicating that Fbxl18 is an authentic E3 ubiquitin ligase component (Fig. 3C). Reciprocal coimmunoprecipitation studies demonstrated that Morf4l1 interacts with SCF^{Fbxl18} components (Fig. 3D). Deletion of the first 150 residues in the N terminus of Morf4l1 abolished its Fbxl18 binding capacity (Fig. 3E). Primary sequence analysis indicated that in the Morf4l1 N terminus, there exists an IQ motif, a recognized F-box L family protein interaction signature at residues 140 to 141. Substitution of this Q with an A

in Morf4l1 diminished its Fbxl18 binding capacity (Fig. 3E). We next tested the vulnerability of the Morf4l1 V5-K143R mutant versus wild-type Morf4l1 to Fbxl18-induced degradation after coexpression of *Morf4l1* and *Fbxl18* plasmids in cells. Cellular expression of a *Morf4l1* V5-K143R mutant plasmid in cells encoded a protein variant that exhibited resistance to Fbxl18-mediated protein degradation (Fig. 3F). Fbxl18 selectively catalyzes wild-type but not K143R Morf4l1 ubiquitination in vitro (Fig. 3G), whereas the unrelated F-box protein Fbxw18 does not catalyze Morf4l1 ubiquitination. Knockdown of endogenous *Fbxl18* by short hairpin RNA (shRNA) stabilized Morf4l1 protein and prevented its degradation (Fig. 3H). Overall, these data demonstrate that SCF^{Fbxl18} is a bona fide E3 ubiquitin ligase complex that interacts through distinct molecular recognition signatures to mediate Morf4l1 ubiquitin-proteasomal degradation. The studies suggest that lung epithelia may utilize the actions of SCF^{Fbxl18} to preserve cellular life span under native conditions as a mechanism for disposal of a potent cytotoxic effector.

The acetyltransferase GCN5 stabilizes Morf4l1

In *P. aeruginosa* infected cells, the protein levels of Morf4l1 and the lysine acetyltransferase GCN5 are up-regulated (Fig. 1E). Inhibition of acetyltransferase activity by the pan-acetyltransferase inhibitor anacardic acid reduced Morf4l1 abundance, whereas the deacetylase inhibitor trichostatin A did not affect Morf4l1 stability (Fig. 4A). Anacardic acid–induced Morf4l1 destabilization can be abolished by addition of the proteasome inhibitor MG132, suggesting that acetylation protects Morf4l1 from ubiquitin proteasomal degradation (Fig. 4A). In separate coimmunoprecipitation studies, Morf4l1 was observed to interact with the acetyltransferase GCN5 (Fig. 4, B and C). GCN5 potently acetylates lysine residues in histone and nonhistone proteins to regulate transcriptional activity (24). Depletion of GCN5 with shRNA enhanced Morf4l1 degradation, and overexpression of GCN5 stabilized Morf4l1 (Fig. 4D). Expression of *Morf4l1* plasmids in cells harboring mutations at putative acetylation sites identified that GCN5 acetylates Morf4l1 at $K1^{43}$, which is also the molecular site for Fbxl18-mediated Morf4l1 polyubiquitination (Figs. 3, F and G, and 4E). This finding suggests that competitive acetylation determines Morf4l1 availability for ubiquitination at this molecular site. Lentiviral gene transfer of wild-type V5-*Morf4l1* or V5-*Morf4l1-K143R* mutant plasmids in lung epithelia showed that *P. aeruginosa* infection effectively triggered increased acetylation of wild-type Morf4l1, which was not observed in the K143R mutant (Fig. 4F). Further, Morf4l1 is stabilized after *P. aeruginosa* infection, but depletion of GCN5 in cells by shRNA abolished the Morf4l1-stabilizing effects of *P. aeruginosa* (Fig. 4G).

Finally, acetylation of Morf4l1 protein is increased by other strains of *P. aeruginosa* and by other bacterial species such as *Escherichia coli* (fig. S2). Together, these data indicate that *P. aeruginosa* triggers GCN5-mediated K^{143} acetylation of Morf4l1, which protects Morf4l1 from ubiquitin proteasomal degradation by SCF^{Fbxl18}. Bacteria-induced Morf4l1 acetylation also appears to be more widespread among bacterial pathogens.

P. aeruginosa infection induces Morf4l1-dependent cell death

To investigate Morf4l1 biological activity, we first evaluated Morf4l1's effect on cell viability and cell cycle progression in lung epithelial cells. Flow cytometric analysis

revealed that overexpression of *Morf4l1* plasmid in cells profoundly triggered cell death (Fig. 5, A to C) by inducing apoptosis and necrosis on the basis of results from staining with annexin V (an apoptotic indicator) (Fig. 5D) and propidium iodide (cell death indicator) (Fig. 5E). We generated deletion mutations of *Morf4l1* and expressed the plasmids by transient transfection to finely map the molecular signatures in Morf4l1 that are sufficient for cell death. We observed that residues 300 to 350 in the C terminus of Morf4l1 are required for its cytotoxicity (Fig. 5F). We next investigated whether *P. aeruginosa* infection–induced cell death is Morf4l1-dependent. We overexpressed or knocked down *Morf4l1* using a lentiviral expression system in cultured lung epithelial cells and challenged the cells with *P. aeruginosa.* The pathogen alone effectively reduced cell viability by ~50% versus uninfected cells (Fig. 5G). Overexpression of *Morf4l1* plasmid in cells accentuated *P. aeruginosa*–induced cell death, whereas knockdown of *Morf4l1* significantly ($P < 0.05$) increased the numbers of viable cells both in the presence and in the absence of bacterial infection. *Morf4l1* silencing not only increased the number of overall viable cells in the absence of bacterial infection but also abolished *P. aeruginosa*–induced cell death (Fig. 5G). To assess the ability of Morf4l1 acetylation to counteract the destabilizing actions of Fbxl18, cells were transfected with *Fbxl18* plasmid and then infected with *P. aeruginosa*. In these studies, increased steady-state immunoreactive Morf4l1 was observed after *P. aeruginosa* treatment despite high levels of Fbxl18 expression (Fig. 5H). These results suggest that *P. aeruginosa*–induced Morf4l1 acetylation may protect the protein from ubiquitination leading to cell death. Further, depletion of endogenous Morf4l1 increases epithelial cell viability, and Morf4l1 is both sufficient and required to mediate cell death after *P. aeruginosa* infection.

Argatroban is a Morf4l1 small molecule antagonist

The above studies led us to explore the possibility of targeting Morf4l1 pharmacologically. Because acetylation of Morf4l1 during bacterial infection prevents its degradation through the proteasome, manipulation of Fbxl18 levels or other strategies to enhance Morf4l1 elimination in cells may not be practical. Because the Morf4l1 crystal structure is available (25–27) and the C terminus is critical to mediate its cytotoxicity (Fig. 5F), we used in silico design with best-fit ligand docking software to screen small molecules that specifically interact with the three-dimensional (3D) structure of this domain. Indeed, the Morf4l1 crystal structure shows a potential docking site for chemical entities (Fig. 6A). Of ~6000 small molecules screened from a library, we obtained a range of small molecules that were predicted to bind to Morf4l1 with high scores in computational analysis. Among these, an FDA-approved thrombin inhibitor, argatroban (1-[5-[(aminoiminomethyl) amino]-1-oxo-2-[[(1,2,3,4-tetrahydro-3-methyl-8 quinolinyl) sulfonyl] amino] pentyl]-4-methyl-2-piperidinecarboxylic acid, monohydrate) (Fig. 6B), interacted with this pocket optimally (Fig. 6C). The 2D diagram illustrates the Morf4l1-argatroban interaction where residues G^{220} and T^{277} are predicted to be essential for drug interaction with coordinating residues L^{287}, L^{274}, and Y^{276}, strengthening the drug-target interaction with the pharmacophore (Fig. 6D). Argatroban binds to Morf4l1 at 60 nM concentration as shown in isothermal calorimetry (ITC) studies (Fig. 6E). It has been reported that Morf4l1 is a component of theNuA4 histone acetyltransferase complex that acetylates histoneH4 and H2A (28). Treatment of cells with argatroban inhibits histone H4K12 and H4K16 acetylation at 100

nM, a concentration similar to its binding dissociation constant (K_d) (Fig. 6F). Further, in the setting of *Morf4l1* plasmid overexpression or *P. aeruginosa* infection of cells, argatroban substantially rescued cell death at similar concentrations (~80 nM) (Fig. 6, G and H). Collectively, these data indicate that argatroban directly inhibits Morf4l1-dependent cytotoxicity at drug concentrations below those used for anticoagulation.

Morf4l1 gene silencing or pharmacologic antagonism ameliorates *P. aeruginosa*–induced lung injury

Because Morf4l1 accumulates in the lung tissues of subjects with pneumonia and induces cell death in lung epithelia, we tested whether modulation of Morf4l1 protein or activity would ameliorate cell death, tissue injury, and survival in experimental pneumonia. We overexpressed *Morf4l1* or depleted *Morf4l1* in C57BL/6J mice using a lentiviral delivery system [10^7 plaque-forming units (pfu) permouse, intratracheally] and challenged the mice with *P. aeruginosa*. *Morf4l1* gene transfer profoundly causes cell death and is rapidly lethal to mice, consistent with our previous observations in cell lines (Fig. 7A). TUNEL (terminal deoxynucleotidyl transferase–mediated deoxyuridine triphosphate nick end labeling) staining revealed extensive cell death in mouse lung tissues from *Morf4l1* 24 hours after transfection in animals (Fig. 7, B and C). *P. aeruginosa* infection [10^4 colony-forming units (cfu) per mouse, intratracheally] likewise resulted in cell death, which was nearly completely suppressed by simultaneous administration of argatroban (5 μg per mouse, intratracheally) or by knockdown of *Morf4l1* in vivo using shRNA (Fig. 7, D and E). Bronchoalveolar lavage fluid from infected animals treated with argatroban or *Morf4l1* shRNA contained reduced protein concentrations and cell numbers compared to control infected animals ($P < 0.05$, Fig. 7F). However, the bacterial loads in bronchoalveolar lavage fluid from the different groups were not altered (fig. S3). Mouse lung tissue homogenates from this experiment were analyzed by immunoblotting, which revealed that Morf4l1 is effectively silenced using *Morf4l1* shRNA and that Morf4l1 depletion or antagonism reduced the cleavage of proinflammatory active caspase 1 and the proapoptotic effector caspase 3 observed with *P. aeruginosa* infection (Fig. 7G). One prominent cell death receptor/ligand pair is the Fas/Fas ligand (FasL) system. We observed that unlike Fas, FasL was up-regulated in *P. aeruginosa*–infected mouse lung tissues, an effect also blocked by Morf4l1 depletion or antagonism (fig. S4). Depletion of Morf4l1 by shRNA or inhibition of Morf4l1 with argatroban markedly increased survival of mice after *P. aeruginosa* infection (10^5 cfu per mouse, intratracheally) ($P < 0.05$, Fig. 7H). As a whole, these results show that chemical or genetic blockade of the chromatin remodeling subunit Morf4l1 reduces cell death and improves survival in a murine model of experimental pneumonia.

Pharmacologic antagonism of Morf4l1 ameliorates LPS-mediated lung injury

To further verify the protective function of argatroban seen in *P. aeruginosa* pneumonia, we tested argatroban in a murine model of LPS-induced ALI. Immediately after administration of LPS (3 mg/kg, intratracheally), mice were intratracheally instilled with vehicle, 5 μg of argatroban, or 5 μg of dabigatran (another direct thrombin inhibitor whose structure is not predicted to interact with Morf4l1). Mice were sacrificed at 3, 6, and 24 hours after exposure, with tissues harvested and TUNEL staining performed to evaluate cell death in the lungs. Figure 8 (A and B) shows TUNEL-positive staining as early as 3 hours after LPS

treatment that intensifies by 24 hours, indicating substantial LPS-mediated cytotoxicity in this lung injury model. Analogous to our observations in the *P. aeruginosa* pneumonia model, the administration of argatroban significantly reduced cell death in the lungs of LPS-exposed mice, and this protection was not observed with dabigatran treatment, suggesting that protection may be due to Morf4l1 antagonism rather than thrombin inhibition ($P < 0.05$, Fig. 8B). We assayed the coagulation parameters prothrombin time and international normalized ratio in these mice to evaluate whether argatroban administration caused systemic anticoagulation effects or whether thrombin inhibition was confounding the cell survival phenotype. The prothrombin time and international normalized ratio values were similar among all groups (Fig. 8C). In a more severe disease model of lung injury, LPS was given at 5 mg/kg, intratracheally, followed by argatroban at 1, 2, or 5 μg, intratracheally, with organ harvest and TUNEL staining 6 hours later. Again, cell death in lung tissues was significantly suppressed by argatroban in a dose-dependent manner ($P < 0.05$; Fig. 8, D and E). In this high-dose LPS–induced ALI model, mice die rapidly with a 50% mortality by 8 hours and a 100% mortality at 10 hours for mice treated with vehicle or dabigatran; argatroban prolongs survival of these LPS-treated mice (Fig. 8F), with five of eight mice alive at the termination of the experiment (24 hours). We evaluated lung tissue homogenates from these animals and examined a panel of cell death–and stress-related proteins and observed suppression of many of these proteins in the setting of argatroban treatment (Fig. 8G). Overall, these data indicate that argatroban protects mice from LPS-induced cell death in ALI through a mechanism that appears distinct from its anticoagulant properties and may involve inhibition of Morf4l1.

DISCUSSION

The results reported here show that the life span of a multifunctional chromatin modulator subunit is extended after microbial infection thereby enhancing its ability to trigger cell death in pneumonia. We discovered a molecular model for host cell death during pulmonary inflammation whereby Morf4l1, highly expressed in humans with pneumonia, is acetylated after bacterial infection. Acetylation diverts it from constitutive degradation mediated by a previously undescribed SCF E3 component, Fbxl18. By using computer-based molecular docking simulations, we identified and tested an FDA-approved chemical entity that abrogates inflammatory injury and cell death with prolonged survival in experimental pneumonia and endotoxin-mediated lung injury. These results underscore a potentially important pathway whereby a pathogen disrupts cellular viability during infection and also provides a potential mechanistic platform for targeted intervention (fig. S5). The ability of the anticoagulant argatroban (Acova) to disable Morf4l1 and lessen the severity of pulmonary injury highlights the potential use of structure-based analysis for repurposing FDA-approved drugs as a means to develop new non–antibiotic-based therapies (29). Whether or not argatroban is effective in preserving cellular viability in other disease models will require additional preclinical testing.

The cellular concentrations of Morf4l1 are presumably tightly controlled in living cells, with an increase in accumulation after *P. aeruginosa* infection or exposure to endotoxin. Among other bacterial virulence effector pathways, the data here show that the pathogen increases the concentration of Morf4l1, which, through its C terminus, is sufficient to delay cell cycle

entry and trigger cell death in host cells. The observation that Morf4l1 is sufficient to increase TUNEL staining in tissue and cells coupled with the appearance of cleaved caspase 1 and 3 suggests the activation of caspase-activated deoxyribonuclease, a process strongly implicating an apoptotic pathway (30). Our findings showing that ectopically expressed Morf4l1 can trigger cell death stand in distinct contrast with prior studies indicating that Morf4l1 promotes cell cycle progression and cell proliferation, but are concordant with other studies showing that Morf4l1 knockdown enhances cell survival in the setting of toxin exposure (16–18). This discrepancy could be explained either by unique mechanistic responses to the effects of this protein in lung epithelia versus other mammalian cell types or by the ability of ectopically expressed *Morf4l1* to modulate the levels, activity, or occupancy of endogenous Morf4l1 or an unidentified protein in cell complexes that drive cell proliferation. The embryonic lethality of *Morf4l1* knockout mice that have impaired cell proliferation may be due to the loss of Morf4l1 proapoptotic effects in subpopulations of cells that provide a permissive environment for organogenesis to ensue (15). However, the potent ability of ectopically expressed *Morf4l1* to induce cell death both in lung tissue and in an SV40-transformed murine lung epithelial cell line, paired with partial reversal of this phenotype with *Morf4l1* endogenous gene silencing or pharmacologic antagonism, supports its unique death effector function.

Because Morf4l1 forms stable complexes with chromatin-modifying enzymes and interacts with retinoblastoma protein (31), it is possible that a by-product of elevated levels of this protein involves modulation of transcriptional networks involved in inflammation or cell death. Indeed, the ability of deacetylase inhibitors to modulate pulmonary inflammatory responses after endotoxin exposure supports our findings that altered concentrations or activities of chromatin-associated components such as Morf4l1 are pathophysiologically regulated by bacterial factors (32). Although Morf4l1 levels are induced after *P. aeruginosa* infection, its mode of elimination resembles that of a related protein, Morf4, which is constitutively disposed of through the ubiquitin proteasome (33). Identifying the mechanisms whereby Morf4-related proteins are eliminated by ubiquitin-dependent processing is important, given their cytotoxic behavior even at low concentrations (33). Fbxl18 was identified in a recent adaptor capture proteomic study (34). Here, we validate that Morf4l1 is a substrate of Fbxl18 in the SCF complex. Morf4l1 itself is not an acetyltransferase per se, and its acetylation is catalyzed by GCN5 to enhance its stability. Our results suggest intermolecular competition at a single residue, K^{143}, between acetylation that stabilizes Morf4l1 and destabilizing polyubiquitination mediated by SCF^{Fbxl18}. In one scenario, it is possible that *P. aeruginosa* infection triggers nuclear relocation of Morf4l1 through its acetylation and bipartite nuclear localization signals to escape from SCF^{Fbxl18} ubiquitin proteasomal targeting in the cytoplasm. This mode of subcellular control through acetylation has been described for the retinoblastoma protein (35). Hence, the life span of Morf4l1 in epithelia is likely controlled by the relative pool sizes of polyubiquitinated Morf4l1 versus acetylated protein, the latter increasing after some microbial infections.

There are limitations with our study. Our findings in human pneumonia need to be confirmed in studies with greater numbers of subjects adjusted for possible confounding factors such as bacterial etiology, illness severity, and comorbidities. Although here,

Morf4l1 triggers cell death through its posttranslational modification, confirmation of this would require mass spectrometric methods. Finally, additional studies demonstrating target validation with argatroban are needed to ascertain whether this therapeutic indeed acts through this epigenetic modulator or works indirectly.

The results raise opportunities to consider selective targeting of Morf4l1 pharmaceutically to attenuate inflammatory injury in preclinical studies where retention of cellular viability is paramount. Such approaches could complement existing ARDS cell-based replacement strategies (36). Small molecules targeting chromatin modifiers are currently in preclinical or clinical trials (37, 38). We have uncovered a unique mechanism of action for argatroban, used clinically as an anticoagulant. Argatroban directly binds to the active site of thrombin with an inhibitory constant (K_i) of 40 nM (39). Here, argatroban binds Morf4l1 at similar concentrations (66 nM) as it does thrombin (~40 nM), inhibits Morf4l1 function in the context of complex-mediated histone modification, and prevents Morf4l1- or *P. aeruginosa*–induced cell death in vitro and in vivo. Our effective argatroban dose used in mice equates to about one-tenth of the patient weight–adjusted dosage used in clinical application, and no overt signs of bleeding or coagulopathy were noted in the animals treated. Other preclinical studies show that argatroban reduces inflammation in fatty liver disease, a disorder also characterized by apoptosis, and the drug decreases leukocyte adhesion and improves capillary perfusion (40, 41). It is tempting to speculate that the use of argatroban may be an effective therapy for patients with lung injury given that clinical studies assessing direct thrombin inhibitors in critically ill patients are now under way (NCT01911624). The successful implementation of new or repurposed small molecules active against newly characterized targets will be an interesting area of future study.

MATERIALS AND METHODS

Study design

The objective of this study was to understand the mechanisms whereby bacterial infection or LPS induces cell death in experimental models of pneumonia by modulating Morf4l1 protein stability. We also evaluated a Morf4l1 antagonist in mice to test the hypothesis that this approach would preserve cell viability. In vivo experiments using mice involved at least four to six mice per group as determined by a GraphPad StatMate power analysis, assuming an 80% reduction of mortality with 80% power and an α of 0.05. Mice were randomized into various groups, but the experimenter was not blinded to the identities of individual groups. Animals were not withdrawn from the studies according to predetermined criteria in the Institutional Animal Care and Use Committee (IACUC) protocols, nor were they excluded from any of the analyses.

Bacterial infection

PA103 was inoculated on a tryptic soy broth (TSB) agar plate overnight. Bacteria were collected from the plates and cultured in TSB broth with 5% glycerol until their log phase (optical density, 0.6). Murine lung epithelial cells at 90% confluence were infected with the bacteria at the concentrations indicated.

Animal experiments

Lenti-*Morf1l* viral constructs were generated by PCR. C57BL/6J mice (8 to 10 weeks old, male) were administered lenti-*empty*, lenti-*Morf4l1*, or lenti–*Morf4l1 shRNA* (10^8 pfu per mouse, intratracheally) for 7 days before intratracheal inoculation with *P. aeruginosa* (5×10^4 per animal) for 24 hours. Each group contained five to nine mice. In separate studies, mice were given argatroban (5 μg per mouse, intratracheally) immediately after *P. aeruginosa* inoculation for 24 hours before tissue harvest. Lung tissues from mice were homogenized and sonicated in cell lysis buffer followed by immunoblotting analysis. For survival studies, the lenti-*empty*–, lenti-*Morf4l1*–, lenti-*Morf4l1 shRNA*–, or argatroban-treated (5 μg per mouse, intratracheally) animals were inoculated with *P. aeruginosa* (5×10^5 per animal) for 24 hours, with survival assessed daily. LPS was administered intratracheally into mice at 3 or 5 mg/kg for different experiments, followed immediately with argatroban (0 to 5 μg per mouse, intratracheally) or dabigatran (5 μg per mouse, intratracheally), and mice were euthanized as indicated. In some studies, lungs were processed for hematoxylin and eosin and TUNEL staining by the Starzl Transplantation Institute Core Facilities. All procedures were done in accordance with approved protocols from the University of Pittsburgh IACUC.

Human samples

Human lung samples were obtained from the University of Pittsburgh Health Sciences Tissue Bank as described previously (42). The control subjects' ages ranged from 50 to 62 years, whereas in pneumonia subjects, the ages ranged from 12 to 60 years. All subjects were Caucasian. The study was approved both by the University of Pittsburgh Tissue Utilization Committee and Institutional Review Board.

Plasmid construction, mRNA, and mutagenesis

Morf4l1 was cloned into pcDNA 3.1 and lentiviral expression vectors by PCR using kits from Invitrogen and the Morf4l1 cDNA as a template with the following primers: forward primer, 5′-ATGGCGCCGAAGCAGGA-CCCG-3′; reverse primer, 5′-CACAGCTTTCCGATGGTACTCAGG-3′. N-terminal truncations of Morf4l1 were generated by PCR using appropriate primers as described (23). The levels of steady-state mRNA were assayed by cellular RNA extraction and cDNA preparation (Qiagen) before qPCR was performed with a SYBR Green reporter in a Bio-Rad CFX96 Real-Time System Analyzer. Site-directed mutagenesis of lysine and serine residues in Morf4l1 was carried out using a mutagenesis kit (Promega).

Statistics

Descriptive statistics were reported with mean ± SEM for continuous variables. All data were statistically analyzed by nonparametric methods: Mann-Whitney *U* test, Kruskal-Wallis equality-of-populations rank test, and log-rank test where appropriate to compare multiple groups within and between experiments. By using nonparametric methods rather than parametric tests, we are able to avoid the possible error by assuming normality of data and be more conservative to determine statistical significance. The effect size was determined on the basis of pilot studies and prior work involving murine infection models.

Kaplan-Meier survival curves were generated for animal studies. All analyses were performed using Stata Statistical Software Release 10.1 (StataCorp).

Supplementary Material

Refer to Web version on PubMed Central for supplementary material.

Acknowledgments

Funding: This work was supported, in part, by NIH grants HL096376, HL097376, HL098174, HL081784, P01 HL114453 (to R.K.M.), HL116472 (to B.B.C.), HL125435 (to C.Z.), and P30 DK72506. This work was also supported by the Office of Research and Development, Veterans Health Administration, U.S. Department of Veterans Affairs, with a Merit Review Award. S.X. was supported by grants from the Ministry of Science and Technology of China (2012ZX09103-301-033 and 2012ZX09202-301-001), the Natural Science Foundation of China (30873082), and the Major Biotech Industrialization Projects from the Guangzhou Municipal Science and Technology Bureau (2010U1-E00541). Y.C. was supported by the Natural Science Foundation of China (81070039 and 81270100).

REFERENCES AND NOTES

1. Meduri GU, Reddy RC, Stanley T, El-Zeky F. Pneumonia in acute respiratory distress syndrome. A prospective evaluation of bilateral bronchoscopic sampling. Am. J. Respir. Crit. Care Med. 1998; 158:870–875. [PubMed: 9731019]
2. Ibrahim EH, Ward S, Sherman G, Kollef MH. A comparative analysis of patients with early-onset vs late-onset nosocomial pneumonia in the ICU setting. Chest. 2000; 117:1434–1442. [PubMed: 10807834]
3. Galani V, Tatsaki E, Bai M, Kitsoulis P, Lekka M, Nakos G, Kanavaros P. The role of apoptosis in the pathophysiology of acute respiratory distress syndrome (ARDS): An up-to-date cell-specific review. Pathol. Res. Pract. 2010; 206:145–150. [PubMed: 20097014]
4. Eskandarian HA, Impens F, Nahori M-A, Soubigou G, Coppée J-Y, Cossart P, Hamon MA. A role for SIRT2-dependent histone H3K18 deacetylation in bacterial infection. Science. 2013; 341:1238858. [PubMed: 23908241]
5. Choudhary C, Kumar C, Gnad F, Nielsen ML, Rehman M, Walther TC, Olsen JV, Mann M. Lysine acetylation targets protein complexes and co-regulates major cellular functions. Science. 2009; 325:834–840. [PubMed: 19608861]
6. Goldberg AD, Allis CD, Bernstein E. Epigenetics: A landscape takes shape. Cell. 2007; 128:635–638. [PubMed: 17320500]
7. Bertram MJ, Pereira-Smith OM. Conservation of the *MORF4* related gene family: Identification of a new chromo domain subfamily and novel protein motif. Gene. 2001; 266:111–121. [PubMed: 11290425]
8. Manzur A, Tubau F, Pujol M, Calatayud L, Dominguez MA, Peña C, Sora M, Gudiol F, Ariza J. Nosocomial outbreak due to extended-spectrum-β-lactamase- producing *Enterobacter cloacae* in a cardiothoracic intensive care unit. J. Clin. Microbiol. 2007; 45:2365–2369. [PubMed: 17581932]
9. Yochum GS, Ayer DE. Role for the mortality factors MORF4, MRGX, and MRG15 in transcriptional repression via associations with Pf1, mSin3A, and transducin-like enhancer of split. Mol. Cell Biol. 2002; 22:7868–7876. [PubMed: 12391155]
10. Pardo PS, Leung JK, Lucchesi JC, Pereira-Smith OM. MRG15, a novel chromodomain protein, is present in two distinct multiprotein complexes involved in transcriptional activation. J. Biol. Chem. 2002; 277:50860–50866. [PubMed: 12397079]
11. Tominaga K, Pereira-Smith OM. The genomic organization, promoter position and expression profile of the mouse MRG15 gene. Gene. 2002; 294:215–224. [PubMed: 12234683]
12. Olgun A, Aleksenko T, Pereira-Smith OM, Vassilatis DK. Functional analysis of *MRG-1*: The ortholog of human MRG15 in *Caenorhabditis elegans*. J. Gerontol. A Biol. Sci. Med. Sci. 2005; 60:543–548. [PubMed: 15972600]

13. Bian M, Fu J, Yan Y, Chen Q, Yang C, Shi Q, Jiang Q, Zhang C. Short exposure to paclitaxel induces multipolar spindle formation and aneuploidy through promotion of acentrosomal pole assembly. Sci. China Life Sci. 2010; 53:1322–1329. [PubMed: 21046324]
14. Garcia SN, Kirtane BM, Podlutsky AJ, Pereira-Smith OM, Tominaga K. *Mrg15* null and heterozygous mouse embryonic fibroblasts exhibit DNA-repair defects post exposure to γ ionizing radiation. FEBS Lett. 2007; 581:5275–5281. [PubMed: 17961556]
15. Tominaga K, Kirtane B, Jackson JG, Ikeno Y, Ikeda T, Hawks C, Smith JR, Matzuk MM, Pereira-Smith OM. MRG15 regulates embryonic development and cell proliferation. Mol. Cell Biol. 2005; 25:2924–2937. [PubMed: 15798182]
16. Chen M, Takano-Maruyama M, Pereira-Smith OM, Gaufo GO, Tominaga K. MRG15, a component of HAT and HDAC complexes, is essential for proliferation and differentiation of neural precursor cells. J. Neurosci. Res. 2009; 87:1522–1531. [PubMed: 19115414]
17. Chen M, Pereira-Smith OM, Tominaga K. Loss of the chromatin regulator MRG15 limits neural stem/progenitor cell proliferation via increased expression of the p21 Cdk inhibitor. Stem Cell Res. 2011; 7:75–88. [PubMed: 21621175]
18. Liang Y, Lin JC, Wang K, Chen YJ, Liu HH, Luan R, Jiang S, Che T, Zhao Y, Li DF, Wang DC, Guo L, Sun H. A nuclear ligand MRG15 involved in the proapoptotic activity of medicinal fungal galectin AAL (*Agrocybe aegerita lectin*). Biochim. Biophys. Acta. 2010; 1800:474–480. [PubMed: 20122994]
19. Grönroos E, Hellman U, Heldin C-H, Ericsson J. Control of Smad7 stability by competition between acetylation and ubiquitination. Mol. Cell. 2002; 10:483–493. [PubMed: 12408818]
20. Weathington NM, Mallampalli RK. Emerging therapies targeting the ubiquitin proteasome system in cancer. J. Clin. Invest. 2014; 124:6–12. [PubMed: 24382383]
21. Cardozo T, Pagano M. The SCF ubiquitin ligase: Insights into a molecular machine. Nat. Rev. Mol. Cell Biol. 2004; 5:739–751. [PubMed: 15340381]
22. Chen BB, Coon TA, Glasser JR, McVerry BJ, Zhao J, Zhao Y, Zou C, Ellis B, Sciurba FC, Zhang Y, Mallampalli RK. A combinatorial F box protein directed pathway controls TRAF stability to regulate inflammation. Nat. Immunol. 2013; 14:470–479. [PubMed: 23542741]
23. Zou C, Chen Y, Smith RM, Snavely C, Li J, Coon TA, Chen BB, Zhao Y, Mallapalli RK. SCF^{Fbxw15} mediates histone acetyltransferase binding to origin recognition complex (HBO1) ubiquitin-proteasomal degradation to regulate cell proliferation. J. Biol. Chem. 2013; 288:6306–6316. [PubMed: 23319590]
24. Imoberdorf RM, Topalidou I, Strubin M. A role for gcn5-mediated global histone acetylation in transcriptional regulation. Mol. Cell Biol. 2006; 26:1610–1616. [PubMed: 16478983]
25. Zhang P, Du J, Sun B, Dong X, Xu G, Zhou J, Huang Q, Liu Q, Hao Q, Ding J. Structure of human MRG15 chromo domain and its binding to Lys36-methylated histone H3. Nucleic Acids Res. 2006; 34:6621–6628. [PubMed: 17135209]
26. Zhang P, Zhao J, Wang B, Du J, Lu Y, Chen J, Ding J. The MRG domain of human MRG15 uses a shallow hydrophobic pocket to interact with the N-terminal region of PAM14. Protein Sci. 2006; 15:2423–2634. [PubMed: 17008723]
27. Kumar GS, Xie T, Zhang Y, Radhakrishnan I. Solution structure of the mSin3A PAH2-Pf1 SID1 complex: A Mad1/Mxd1-like interaction disrupted by MRG15 in the Rpd3S/Sin3S complex. J. Mol. Biol. 2011; 408:987–1000. [PubMed: 21440557]
28. Peña AN, Tominaga K, Pereira-Smith OM. MRG15 activates the cdc2 promoter via histone acetylation in human cells. Exp. Cell Res. 2011; 317:1534–1540. [PubMed: 21324423]
29. Huang R, Southall N, Wang Y, Yasgar A, Shinn P, Jadhav A, Nguyen D-T, Austin CP. The NCGC Pharmaceutical Collection: A comprehensive resource of clinically approved drugs enabling repurposing and chemical genomics. Sci. Transl. Med. 2011; 3:80ps16.
30. Kroemer G, Galluzzi L, Vandenabeele P, Abrams J, Alnemri ES, Baehrecke EH, Blagosklonny MV, El-Deiry WS, Golstein P, Green DR, Hengartner M, Knight RA, Kumar S, Lipton SA, Malorni W, Nuñez G, Peter ME, Tschopp J, Yuan J, Piacentini M, Zhivotovsky B, Melino G. Classification of cell death: Recommendations of the Nomenclature Committee on Cell Death 2009. Cell Death Differ. 2009; 16:3–11. [PubMed: 18846107]

31. Garcia SN, Pereira-Smith O. MRGing chromatin dynamics and cellular senescence. Cell Biochem. Biophys. 2008; 50:133–141. [PubMed: 18231726]
32. Ni Y-F, Wang J, Yan X-L, Tian F, Zhao J-B, Wang Y-J, Jiang T. Histone deacetylase inhibitor, butyrate, attenuates lipopolysaccharide-induced acute lung injury in mice. Respir. Res. 2010; 11:33. [PubMed: 20302656]
33. Tominaga K, Tominaga E, Ausserlechner MJ, Pereira-Smith OM. The cell senescence inducing gene product MORF4 is regulated by degradation via the ubiquitin/proteasome pathway. Exp. Cell Res. 2010; 316:92–102. [PubMed: 19769966]
34. Tan M-KM, Lim H-J, Bennett EJ, Shi Y, Harper JW. Parallel SCF adaptor capture proteomics reveals a role for SCF^{FBXL17} in NRF2 activation via BACH1 repressor turnover. Mol. Cell. 2013; 52:9–24. [PubMed: 24035498]
35. Pickard A, Wong P-P, McCance DJ. Acetylation of Rb by PCAF is required for nuclear localization and keratinocyte differentiation. J. Cell Sci. 2010; 123:3718–3726. [PubMed: 20940255]
36. Gotts JE, Matthay MA. Mesenchymal stem cells and acute lung injury. Crit. Care Clin. 2011; 27:719–733. [PubMed: 21742225]
37. Manzo F, Tambaro FP, Mai A, Altucci L. Histone acetyltransferase inhibitors and preclinical studies. Expert Opin. Ther. Pat. 2009; 19:761–774. [PubMed: 19473103]
38. Kazantsev AG, Thompson LM. Therapeutic application of histone deacetylase inhibitors for central nervous system disorders. Nat. Rev. Drug Discov. 2008; 7:854–868. [PubMed: 18827828]
39. Alban S. Pharmacological strategies for inhibition of thrombin activity. Curr. Pharm. Des. 2008; 14:1152–1175. [PubMed: 18473863]
40. Kassel KM, Sullivan BP, Cui W, Copple BL, Luyendyk JP. Therapeutic administration of the direct thrombin inhibitor argatroban reduces hepatic inflammation in mice with established fatty liver disease. Am. J. Pathol. 2012; 181:1287–1295. [PubMed: 22841818]
41. Fuchs C, Ladwig E, Zhou J, Pavlovic D, Behrend K, Whynot S, Hung O, Murphy M, Cerny V, Lehmann C. Argatroban administration reduces leukocyte adhesion and improves capillary perfusion within the intestinal microcirculation in experimental sepsis. Thromb. Haemost. 2010; 104:1022–1028. [PubMed: 20806115]
42. Chen BB, Coon TA, Glasser JR, Zou C, Ellis B, Das T, McKelvey AC, Rajbhandari S, Lear T, Kamga C, Shiva S, Li C, Pilewski JM, Callio J, Chun CT, Ray A, Ray P, Tyurina YY, Kagan VE, Mallampalli RK. E3 ligase subunit Fbxo15 and PINK1 kinase regulate cardiolipin synthase 1 stability and mitochondrial function in pneumonia. Cell Rep. 2014; 7:476–487. [PubMed: 24703837]

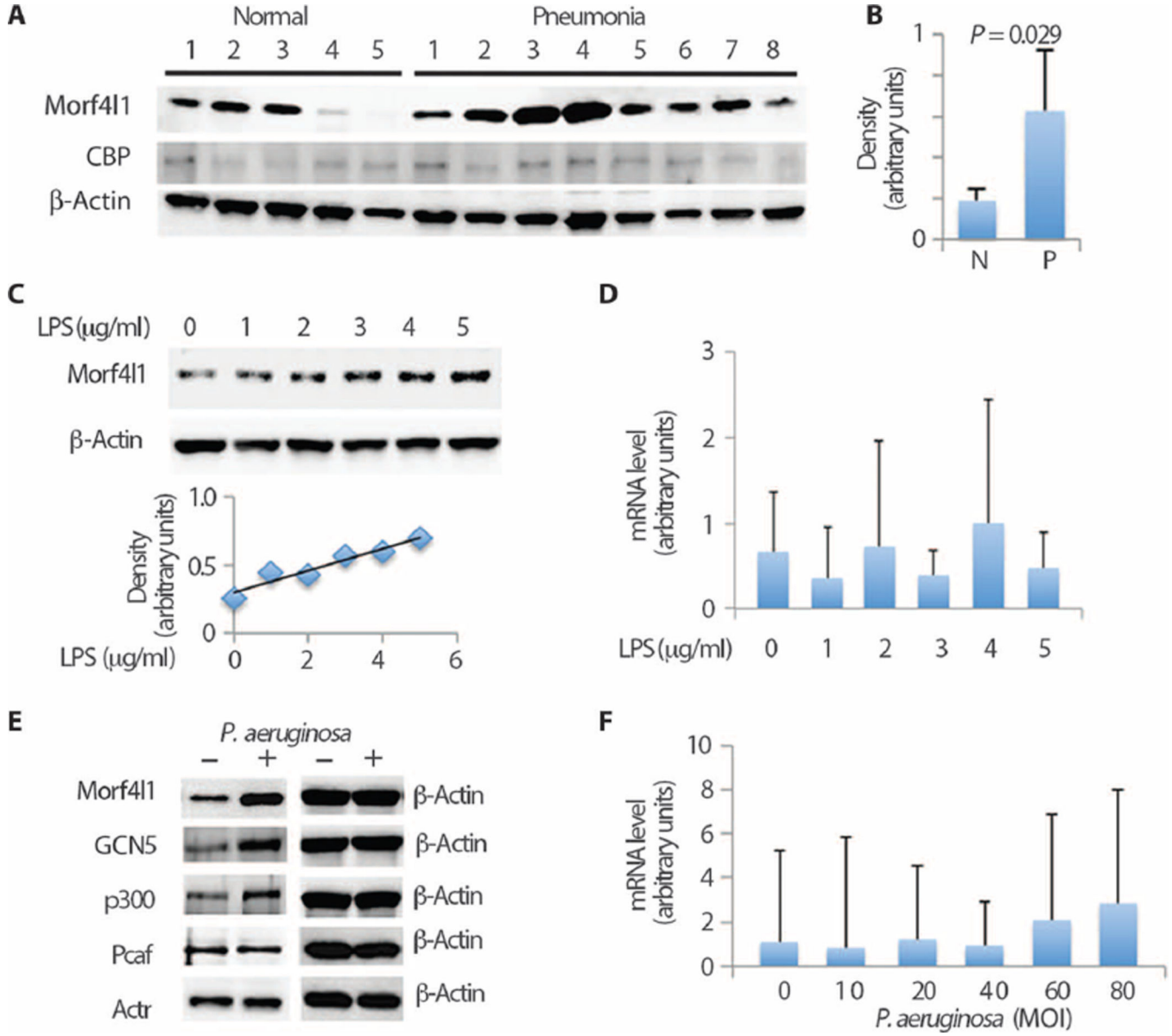

Fig. 1. Morf4l1 accumulates in pneumonia

(**A**) Human lung tissues from patients with pneumonia (n = 8) and healthy patients (normal; n = 5) were analyzed for Morf4l1 protein expression by immunoblotting. β-Actin was used as a loading control. (**B**) Results of the densitometric analysis of bands from immunoblots. P = 0.029 versus normal tissue by the Mann-Whitney U test. N, normal; P, pneumonia. (**C**) Murine lung epithelial cells were exposed to various concentrations of LPS for 2 hours, and Morf4l1 was assayed by immunoblotting. (**D**) Steady-state levels of *Morf4l1* mRNA determined by quantitative polymerase chain reaction (qPCR) after LPS exposure. (**E**) Murine lung epithelial cells were infected with *P. aeruginosa* strain 103 (PA103) at an MOI of 10 for 2 hours, and immunoreactivity of Morf4l1 or acetyltransferases was assayed by immunoblotting. (**F**) Steady-state levels of *Morf4l1* mRNA determined by qPCR after 2

hours of infection with various MOI of PA103. Data in (B), (D), and (F) represent means ± SEM. Each panel in (B) to (F) represents at least $n = 3$ independent experiments.

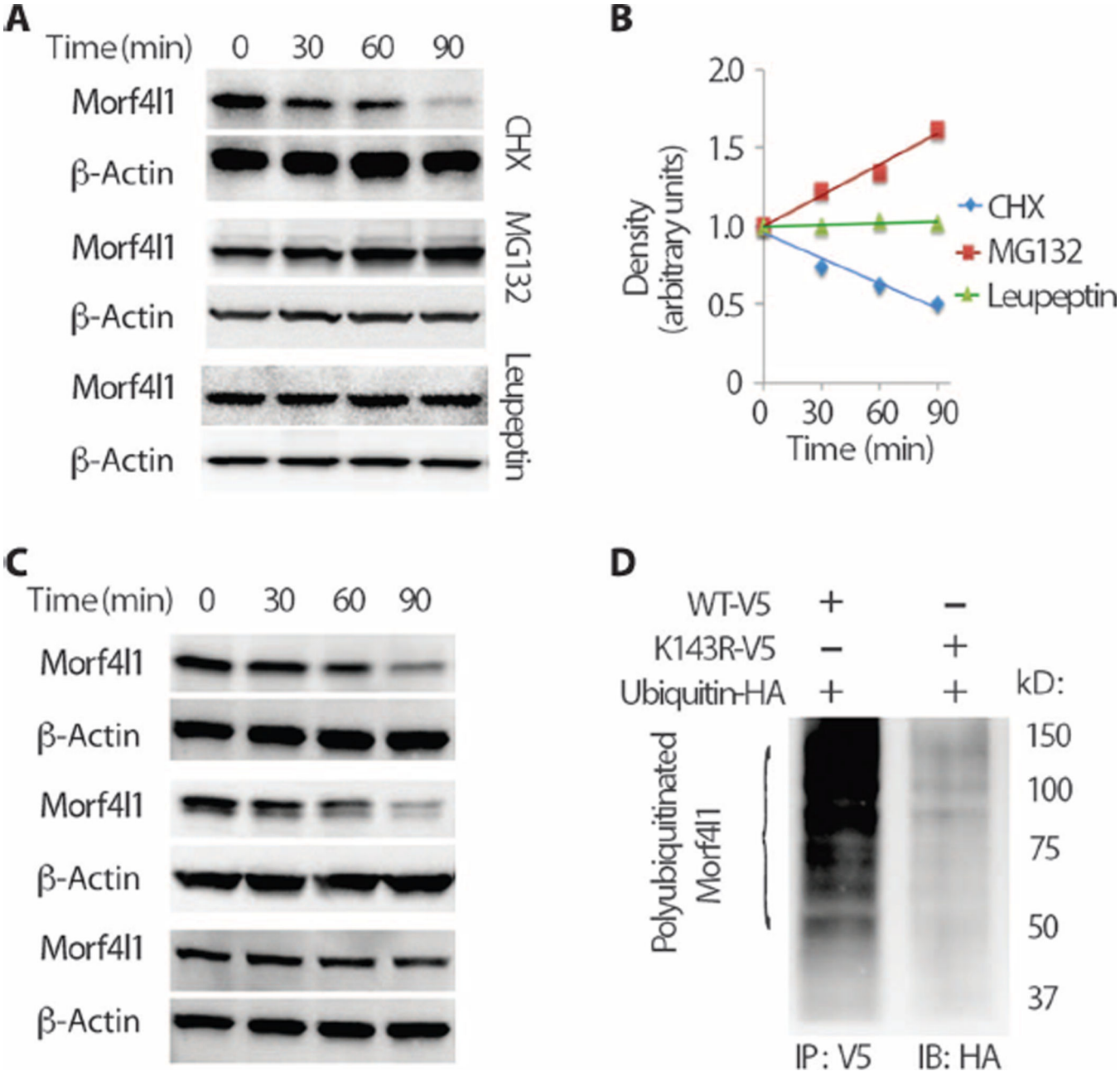

Fig. 2. Morf4l1 is a labile protein degraded by the ubiquitin proteasome

(**A**) Murine lung epithelial cells were exposed to cycloheximide (CHX) alone or in combination with the proteasome inhibitor MG132 or the lysosomal inhibitor leupeptin for various times, and Morf4l1 was assayed by immunoblotting. (**B**) Results of the densitometric analysis of bands from immunoblots from (A). (**C**) Cells were transfected with wild-type (WT) V5-*Morf4l1* or one of two V5-tagged *Morf4l1* point Lys mutant plasmids (K136R, middle panels, or K143R, lower panels), and cells were exposed to CHX. Shown are the protein decay kinetics of WT and Morf4l1 mutant proteins. (**D**) Murine lung epithelial cells were transfected with WT V5-*Morf4l1* (WT-V5) or a V5-tagged *Morf4l1* point mutant plasmid (K143R mutant) (K143R-V5). Cell lysates were subjected to

coimmunoprecipitation by immunoprecipitating (IP) proteins with V5 antibody followed by HA immunoblotting (IB). Shown is ubiquitination of Morf4l1-expressed proteins. Data in each panel represent $n = 3$ independent experiments. HA, hemagglutinin.

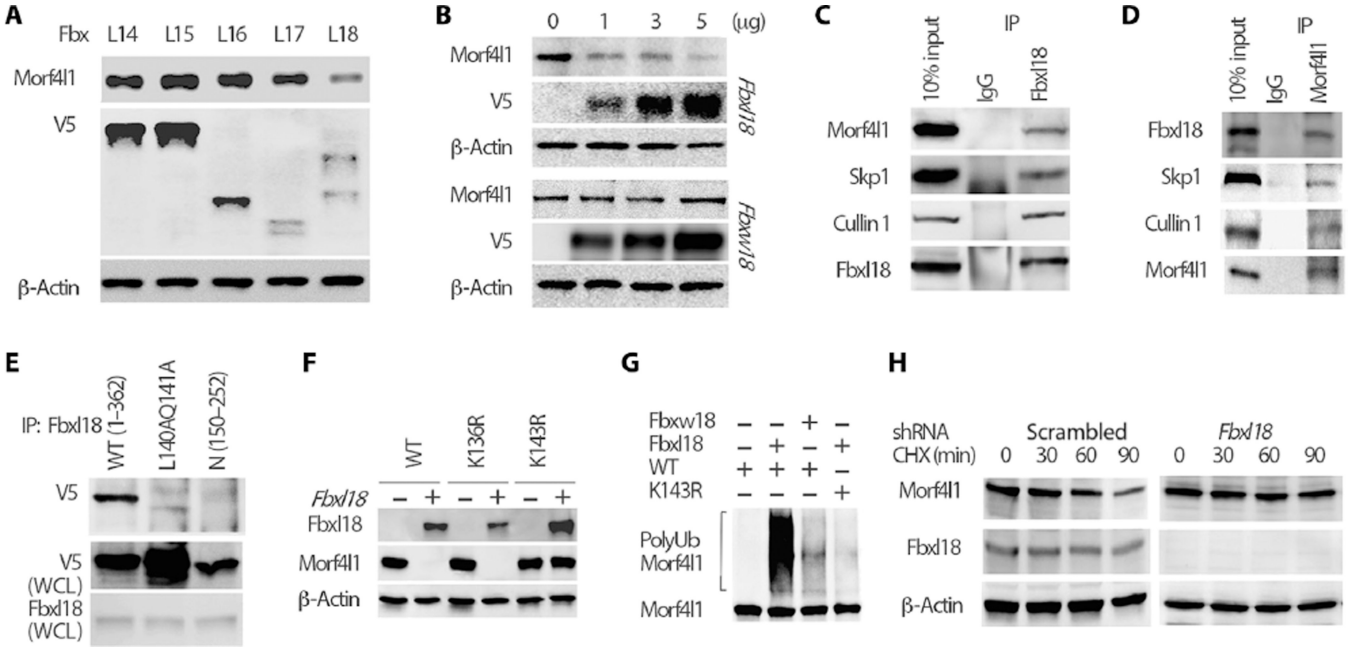

Fig. 3. SCF^{Fbxl18} binds to Morf4l1 to mediate its polyubiquitination and degradation

(**A**) Murine lung epithelial cells were transfected with one of several V5-tagged plasmids encoding F-box proteins. The top panel shows the effects of various expressed plasmids on immunoreactive Morf4l1 levels in cells. The middle panel shows the relative cellular protein expression of plasmids by V5 immunoblotting, and the bottom panel shows β-actin. (**B**) Cells were transfected with various amounts of *Fbxl18* or *Fbxw18* plasmids. Shown are the results of the densitometric analysis of Morf4l1 bands from immunoblots after plasmid transfection. (**C** and **D**) Coimmunoprecipitation studies showing the interaction of Fbxl18 with complexes containing Morf4l1 and SCF E3 ligase components Skp1 and Cullin1. In the left panel, endogenous Fbxl18 was subjected to coimmunoprecipitation followed by immunoblotting with the indicated antibodies. In the right panel, endogenous Morf4l1 was subjected to immunoprecipitation followed by immunoblotting with the indicated antibodies. IgG, immunoglobulin G. (**E**) Cells were transfected with full-length WT V5-*Morf4l1*, a *Morf4l1* N-terminal truncation plasmid (encoding residues 150 to 362), or a V5-tagged *Morf4l1* double point mutant plasmid where leucine and glutamine in an IQ F-box motif were substituted with an alanine. After transfection, cell lysates were subjected to coimmunoprecipitation with Fbxl18 antibody followed by V5 immunoblotting. The top panel shows that, unlike WT Morf4l1, the expressed mutant proteins lack the ability to interact with the F-box protein. The middle and bottom panels show the relative expression of V5 proteins or Fbxl18 in cell lysates, respectively. WCL, whole cell lysate. (**F**) Cells were cotransfected with full-length WT V5-*Morf4l1* or V5-tagged *Morf4l1* point mutant plasmids with or without *Fbxl18* plasmid. Shown in the top panel is the relative expression of Fbxl18 protein. The middle panel shows the levels of V5-tagged expressed mutant Morf4l1 proteins, and the bottom panel shows β-actin. (**G**) In vitro ubiquitination of Morf4l1. Shown are the effects of SCF-Fbxl18 on WT or K143R mutant Morf4l1 ubiquitination in vitro. Fbxw18 is a negative control. PolyUb, polyubiquitination. (**H**) Cells were transfected with *Fbxl18* shRNA or control RNA and exposed to CHX. Shown graphically are the decay

kinetics of Morf4l1 after Fbxl18 silencing. The data in each panel represent $n = 3$ independent experiments, except in panel (G) ($n = 1$).

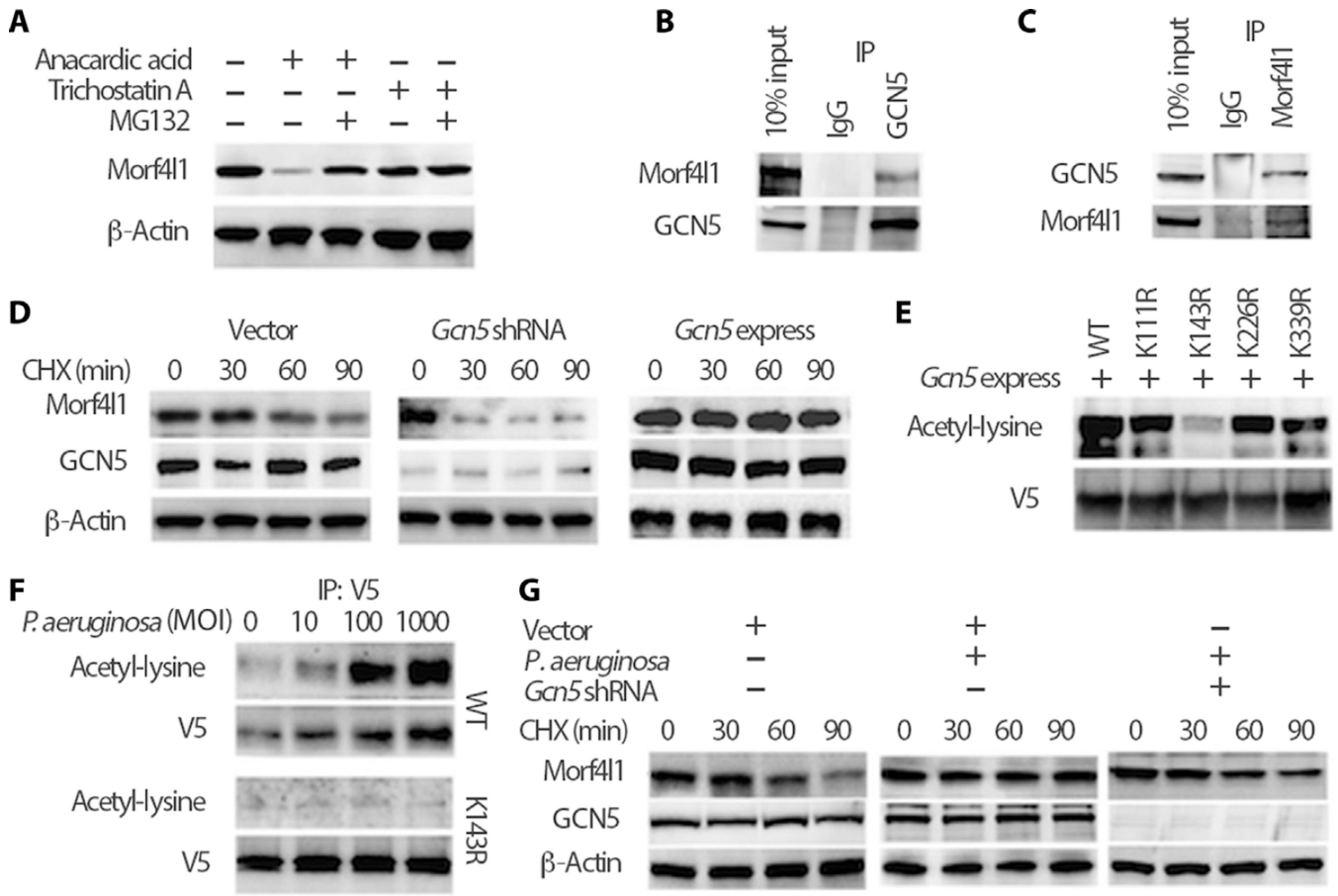

Fig. 4. GCN5 acetylates and stabilizes Morf4l1

(**A**) Murine lung epithelial cells were exposed to anacardic acid (100 μM) to impair acetylation or to trichostatin A (1000 nM) to inhibit deacetylase activity for 4 hours with or without MG132; immunoreactivities of Morf4l1 and β-actin were then assayed. (**B** and **C**) Morf4l1 interaction with GCN5 by coimmunoprecipitation. (**D**) Morf4l1 protein decay is shown after expressing an empty vector or plasmids encoding *Gcn5* or *Gcn5*-silencing plasmids and CHX treatment. Shown are immunoblots of Morf4l1, GCN5, and β-actin. (**E**) Cells were cotransfected with one of several *Morf4l1* point mutant plasmids and *Gcn5* plasmid. The levels of acetylated Morf4l1 are shown in the top panel, and cell lysates probed for V5 by immunoblotting are shown in the bottom panel. (**F**) Cells were transfected with WT V5-*Morf4l1* or V5-*Morf4l1* point mutant plasmid and then infected with *P. aeruginosa* (MOI, 10) to assess acetylated Morf4l1 (top row in each set) or total V5-Morf4l1 protein (bottom row in each set). (**G**) Cells were transfected with an empty vector or *Gcn5* shRNA with *P. aeruginosa* infection (MOI, 10) and exposed to CHX. Shown graphically are the decay kinetics of Morf4l1 after *Gcn5* silencing or bacterial infection. The data in each panel represent $n = 3$ independent experiments.

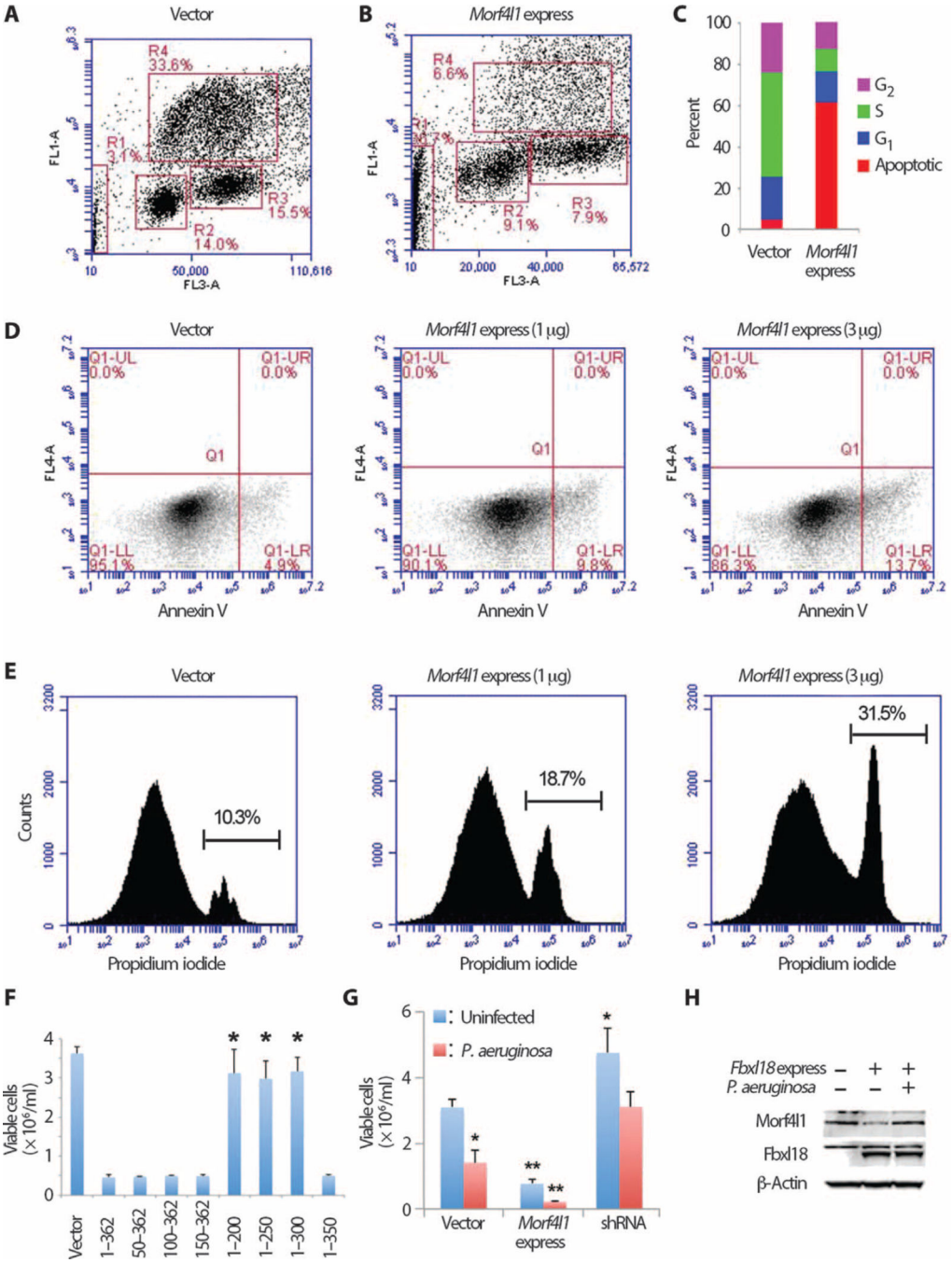

Fig. 5. Morf4l1 mediates *P. aeruginosa*–induced cell death

(**A** to **C**) Fluorescence-activated cell sorting analysis with 5-bromo-2′-deoxyuridine labeling of murine lung epithelial cells after expression of a *pcDNA 3.1* vector (A) or *pcDNA 3.1/ Morf4l1* vector (B); the data were plotted in (C) to show cell cycle progression and apoptosis. (**D** and **E**) Cells were transfected with vector alone or various amounts of *Morf4l1* plasmid and then processed for annexin V staining to assess apoptosis (D) or propidium iodine staining (E) to assess cell viability. (**F**) Cells were transfected with *Morf4l1* deletion plasmids, and the number of viable cells was determined using trypan blue staining. (**G**)

Cells were transfected with an empty vector, a plasmid encoding *Morf4l1*, or *Morf4l1* shRNA and then infected with (or without) *P. aeruginosa* (MOI, 10). Shown are the numbers of viable cells after plasmid expression and infection. Data in (F) and (G) represent means ± SEM. **P* < 0.05 versus 1–362 mutant (F). In (G), **P* < 0.05 versus uninfected vector control or shRNA-infected group, and ***P* < 0.01 versus corresponding shRNA groups by the Mann-Whitney *U* test. (**H**) Immunoblot showing steady-state Morf4l1, Fbxl18, or β-actin protein in cells after transfection with *Fbxl18* plasmid and then infection with *P. aeruginosa* or treatment. Data in each panel represent *n* = 3 independent experiments.

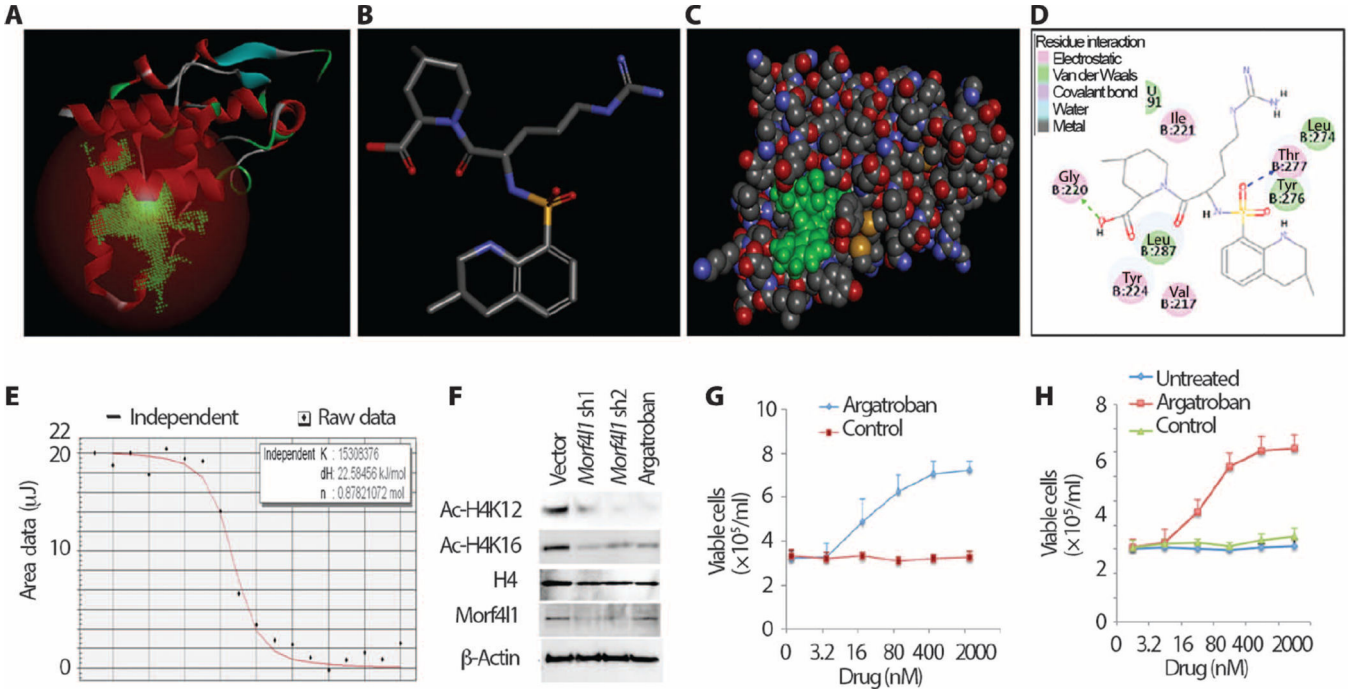

Fig. 6. Argatroban is a potent Morf4l1 inhibitor

(**A**) Morf4l1 crystal structure and potential docking site are shown. (**B**) Chemical structure of argatroban. (**C**) Morf4l1-argatroban docking; the small molecule embedded in Morf4l1 is shown in green. (**D**) A 2D diagram illustrates Morf4l1-argatroban interaction. Specifically, residues Gly^{220} and Thr^{277} within the Morf4-related gene domain (MRG) of Morf4l1 are essential for drug interactions. (**E**) ITC binding assays show argatroban binding to Morf4l1 with high affinity (66 nM). (**F**) Effect of argatroban on Morf4l1 activity (when presented within a protein complex) on acetyl–histone H4 in the cells. (**G** and **H**) Murine lung epithelial cells were transfected with *Morf4l1* plasmid (G) or infected with *P. aeruginosa* (MOI, 10) (H) and then exposed to varying concentrations of argatroban, and effects on cell viability were analyzed. Data in each panel represent $n = 3$ independent experiments.

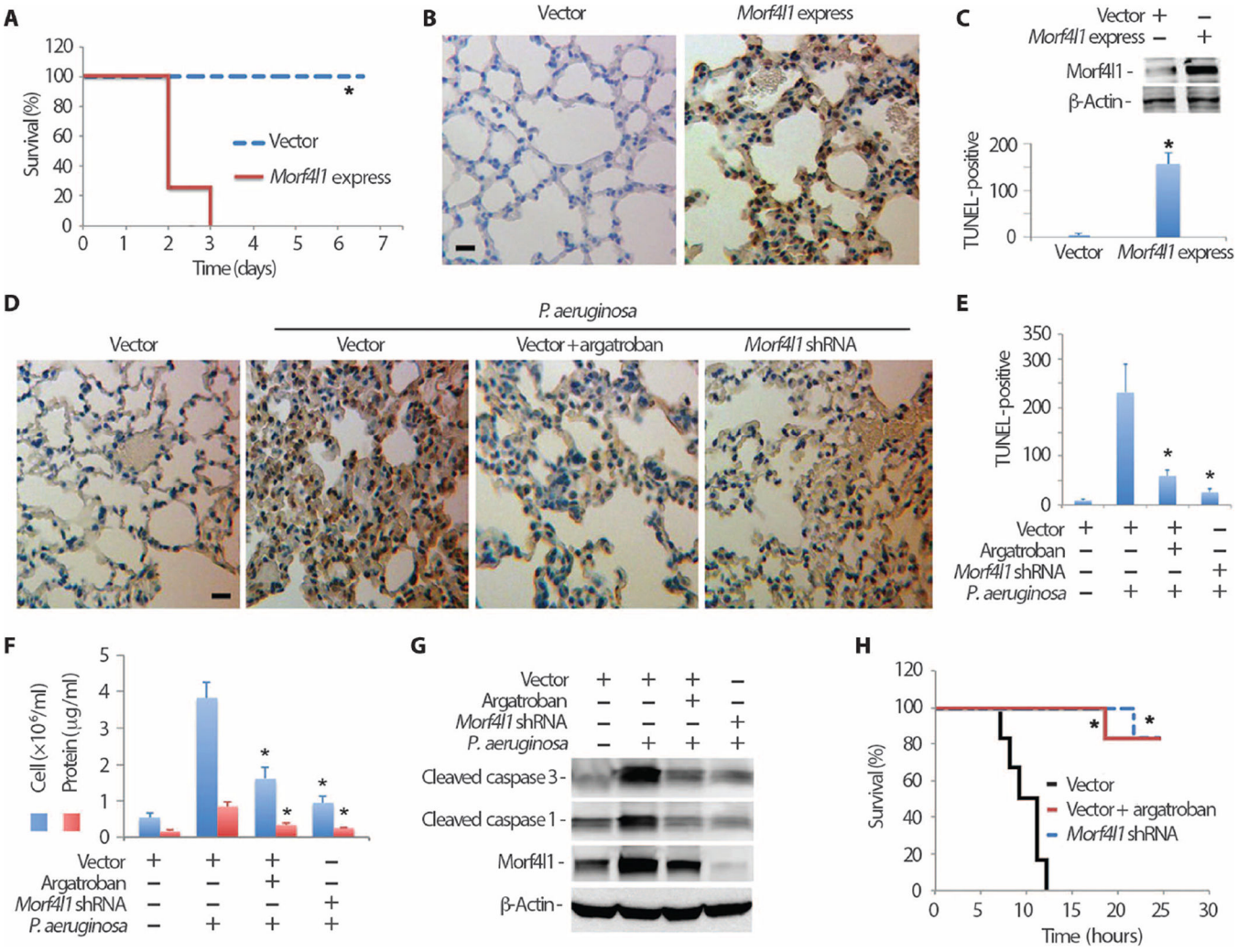

Fig. 7. Morf4l1 depletion or antagonism reduces cell death in experimental pneumonia

(**A**) Kaplan-Meier curves showing mouse survival after empty vector or *Morf4l1* gene transfer in mice ($n = 6$ per group, $^*P = 0.0006$ versus empty vector by the Mann-Whitney U test). (**B** and **C**) Lungs from mice in (A) were processed for TUNEL staining (B), which reveals the number of apoptotic cells (brown cellular staining in each group), and data were quantitated to show number of apoptotic cells in (C). The inset in (C) shows the relative protein expression of Morf4l1 in mouse lung tissue after gene transfer. $^*P < 0.05$ versus empty vector by the Mann-Whitney U test. (**D** and **E**) Gene transfer was conducted in mice ($n = 6$ mice per group) with administration of an empty vector alone or an empty vector or *Morf4l*-silencing vector followed by *P. aeruginosa* infection (10^4 cfu per mouse, intratracheally). Shown in (D) are representative TUNEL stains of lung tissue and quantification of apoptotic cells in (E). A separate group of mice in (D) received argatroban (50 μg, intraperitoneally), and lungs were assessed by TUNEL staining. $P < 0.05$ versus empty vector with PA103 by the Kruskal-Wallis test. (**F** to **H**) Bronchoalveolar lavage from the mice in the above groups was processed for cell counts and protein concentration (F). $^*P < 0.05$ versus empty vector with PA103. (G) The lungs were assayed for immunoreactivity

of Morf4l1 and cleaved caspases. Mouse survival in each group was also determined, and Kaplan-Meier curves are shown in (H). Scale bars, 100 μm. *P = 0.002 versus empty vector.

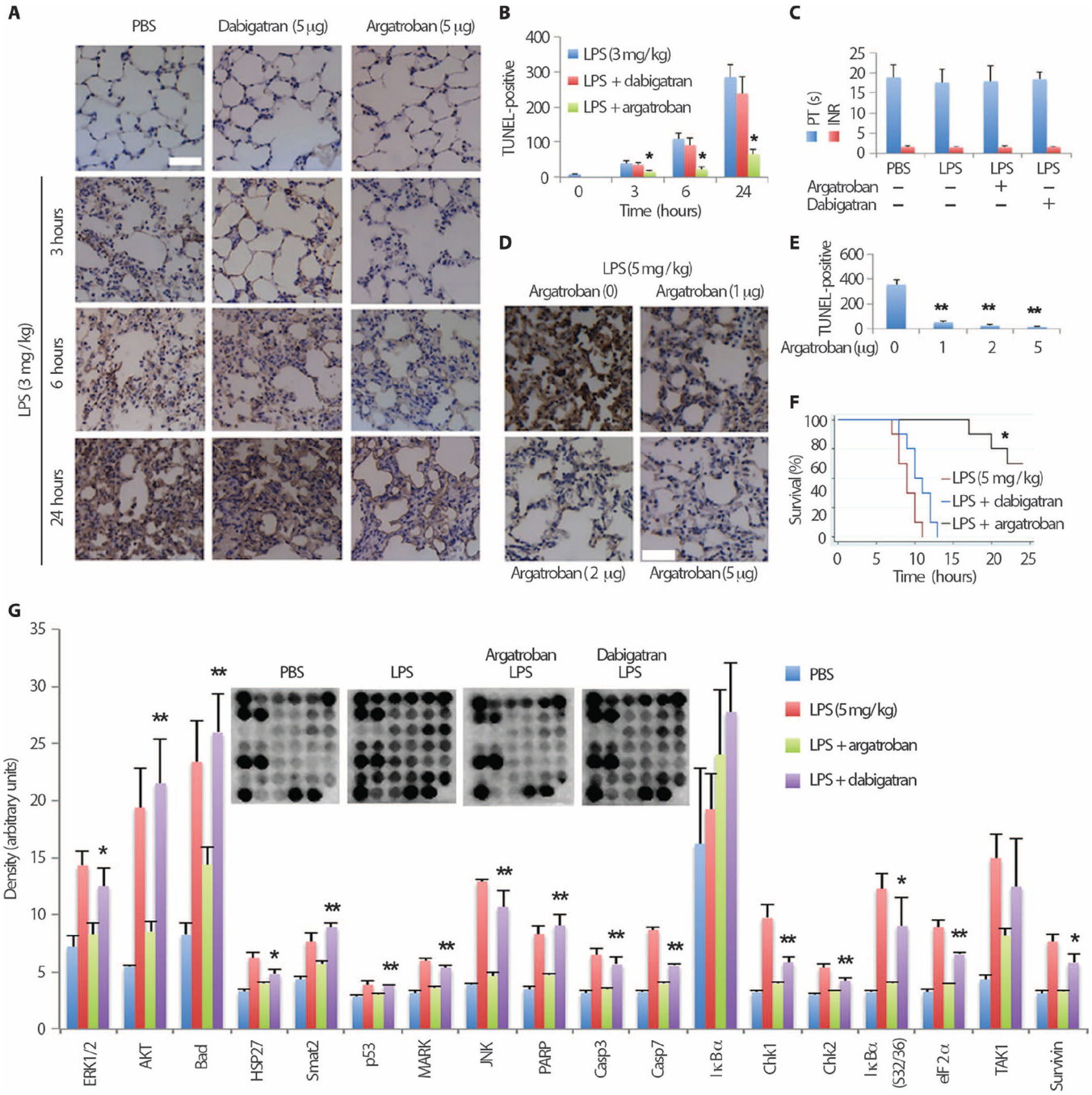

Fig. 8.

Pharmacological antagonism of Morf4l1 ameliorates LPS-mediated lung injury. (**A**) Lungs from mice were processed for TUNEL staining showing the numbers of apoptotic cells (brown cellular staining in each group). Mice were administered LPS (3 mg/kg, intratracheally), followed by phosphate-buffered saline (PBS) (left panels), dabigatran (5 μg per mouse) (middle panels), or argatroban (5 μg per mouse) (right panels). Cell death was monitored at a range of time points as indicated (n = 4 mice per group). (**B**) Data were quantitated to show the numbers of TUNEL-positive cells in (A). *P < 0.05 versus LPS

alone. (**C**) Coagulation parameters prothrombin time (PT) and international normalized ratio (INR) were measured with clinical apparatus following the instructions of the manufacturer (ISTAT). (**D** and **E**) Dose effects of argatroban in LPS-mediated cell death in murine pneumonia. Each group of mice ($n = 4$ per group) was given LPS (5 mg/kg, intratracheally) followed by different amounts of argatroban. Lung tissues were collected at 6 hours for TUNEL staining. Shown in (D) are representative TUNEL stains of lung tissue and quantification of apoptotic cells in (E). ** $P < 0.05$ versus 0 dose argatroban by the Kruskal-Wallis test. (**F**) Kaplan-Meier curves for mice exposed to LPS and treated with dabigatran or argatroban ($n = 8$ animals per group; the experiment was terminated at 24 hours). *$P <$ 0.0001 versus LPS alone by the Kruskal-Wallis test. (**G**) The lungs from (A) were assayed for immunoreactivity of a selected panel of apoptosis and stress proteins, and the inset shows the results of the assay. Densitometry results of each protein were plotted. Scale bars, 100 μm. *$P < 0.05$ and **$P < 0.01$ versus PBS by the Kruskal-Wallis test.